ASTRONOMY & ASTROPHYSICS
SUPPLEMENT SERIES

Astron. Astrophys. Suppl. Ser. **125,** 381-390 (1997)

Active region effects on solar irradiance at Na I D lines

C. Marmolino[1], M. Oliviero[1], G. Severino[2], and L.A. Smaldone[1]

[1] Dipartimento di Scienze Fisiche dell' Università "Federico II", Mostra d' Oltremare pad. 19, I-80125 Napoli, Italy
[2] Osservatorio Astronomico di Capodimonte, Via Moiariello 16, I-80131 Naples, Italy

Received July 9, 1996; accepted January 3, 1997

Abstract. The possibility to detect solar oscillations in the low frequency domain depends crucially on the power contrast among the oscillation signal and other time dependent signals in the same frequency range. The signal to noise ratio is increased by our ability to understand and remove solar sources of noise. In measurements of the mean Doppler velocity shift of the integrated solar disk, the solar noise has a line component spectrum with a major peak at 13.1 days, and a second less prominent peak at 27.2 days. Active region modulation is believed almost completely responsible for this signal.

We develop simulations of the flux and velocity fluctuations produced by different solar active region distributions, based on an analytical description of their action. From a grid of models of active regions and from their spatial distribution over the disk, we calculate the synthetic flux profile in the Na I D_1 line and determine the velocity measure of a resonance spectrometer.

Our velocity results are compared with the offset velocities from the IRIS network. There is a rather good agreement between the observed and computed velocities, and the plage contribution to the noise appears to be dominant. The simulation allows to test calibration procedures and to study the effect on the spurious velocities of different parameters, such as the intensity thresholds used to determine the areas of spots and plages, and the contrast of the active regions. In particular, we find that the inclusion of intrinsic line shifts in plages can change strongly both the amplitude and the shape of the simulated signal, and then may be an important source of uncertainty for the simulation.

Key words: solar activity — solar oscillations — solar rotation — methods: data analysis

Send offprint requests to: G. Severino

1. Introduction

Helioseismology has a recent *past*, when the 5-minute solar oscillations, first observed in the sixties by Leighton, Noyes and Simon, were identified theoretically and observationally as the evanescent photospheric counterpart of the acoustic modes resonating in the underlying convection zone. At *present*, the oscillation frequencies are used to get information on the Sun's interior, like the extension of the convection zone and the internal rotation velocity, whilst other oscillation properties, like phase differences, can be used to diagnose the atmospheric layers. The *future*, which the successful launch of SOHO makes closer, will be probably dominated by the study of low frequency modes, in particular g-modes.

Very recently the detection of a number of g-modes in solar wind measurements done by Ulysses has been reported (Thomson et al. 1995). This kind of measurements needs to be confirmed before being widely accepted. In progress there are both ground and space based experiments to measure solar global modes (see e.g. Fig. 3 in Harvey 1995). In particular we will refer here to the IRIS and GOLF experiments. The IRIS (International Research on the Interior of the Sun) ground-based network for full disk helioseismology (e.g. Fossat 1991; Pallé et al. 1993) is measuring since 1991 the full disk line-of-sight velocity, from the Doppler shift of the sodium D_1 line, over a range of frequencies from 100 μHz, when the atmospheric conditions are good enough, up to about 10 mHz, limited by the photon statistical noise of the sodium resonance cell.

The GOLF (Global Oscillations at Low Frequency) experiment, on board of the satellite SOHO (Solar and Heliospheric Observatory), which was launched on December 2, 1995, will make a definite effort to detect and identify the solar g-modes. The measuring method involves an extension to space of the ground-based technique used by IRIS (Gabriel et al. 1995). The data will be collected continuously for a period of at least two years (hopefully six) over a range of frequencies from 0.1 μHz to 6 mHz, without limitations due to duty cycle and merging problems.

The possibilities of these experiments to detect solar oscillations in the low frequency domain and definitely identify the g-modes depend crucially on the contrast in power between the oscillation signal and other time dependent signals in the same frequency range. This "noise" is partly instrumental and partly of solar origin, therefore the signal to noise ratio could be in principle increased by our ability to understand and remove solar sources of non-oscillatory signals.

Harvey (1985) made an estimate of the background Doppler-shift noise of solar origin in full-disk measurements assuming that it is due to the finite lifetime (evolution) of four velocity fields: granulation, mesogranulation, supergranulation and active regions. The parameters of this model, whose values were derived from high resolution observations, are the rms velocity amplitudes and the lifetimes of the motions. In this way, Harvey got a continuous noise spectrum in which active regions and supergranulation make the largest contribution to the power in the g-mode frequency band ($\nu < 0.1$ mHz), whilst granulation dominates at higher frequencies. In subsequent works, observed power spectra have been used to fit the model parameters, getting different results according to the estimate Of the instrumental contribution to the observed background (Jiménez et al. 1988; Elsworth et al. 1993). A similar noise model has been used by Harvey et al. (1993) to study the solar noise spectrum of chromospheric oscillations, and a more complex model of the irradiance background due to granulation, mesogranulation and supergranulation, based on a numerical simulation of their time evolution, has been proposed by Andersen et al. (1994).

The solar noise spectrum has also a spectral line component. Claverie et al. (1982) established the existence of a 13.1 $\pm$0.2 day signal of amplitude 6.5 m s^{-1} in measurements of the mean Doppler velocity shift of the integrated solar disk. This finding was confirmed by Isaak et al. (1984), who found also a second less prominent peak at a period of 27.2 days, and, later, by Jiménez et al. (1988) and Régulo et al. (1993).

Claverie et al. in their paper suggested a possible explanation of this phenomenon in terms of a rapidly rotating solar core (see also Dicke 1983). On the other hand, taking into account the effect of active regions passing over the solar disk, several authors (Durrant & Schröter 1983; Andersen & Maltby 1983; Edmunds & Gough 1983) have been able to reproduce the observations sufficiently well to establish that active region modulation is almost completely responsible for the observed signal. However, it is not yet clear if the spots or other parts of the active regions make the largest contribution to the velocity signal. Indeed, different simulations of the signal have been based on the plage area (Durrant & Schröter 1983; Herrero et al. 1984), on the sunspot area (Andersen & Maltby 1983; Régulo et al. 1993), on spot and plage area (Edmunds & Gough 1983; Jiménez et al. 1988) and, finally, based on daily magnetograms (Ulrich et al. 1993) and GONG modulation images (Beck et al. 1995).

The agreement with the observations is generally good, but not enough to consider any of these models a completely successful correction of the integrated sunlight observations for the effect of active regions.

The active region noise arises because they may introduce real local velocities contributing to the global average, and because, through both their magnetic fields and thermal structure, they change the integrated profile of the observed lines by an amount that is set by the active region distribution and modulated by solar rotation. In this paper, we model the latter effect, which originates from the different line shapes in magnetic and quiet solar areas. Both sunspots and plages appear darker than the quiet Sun in the sodium D lines at about $\pm$100 mÅ from the line core, where the passbands of the resonant cell are centered, therefore Roger Ulrich has called this effect *magnetic darkening velocity*. We simulated the velocity and flux fluctuations produced by different active region distributions, using an analytical description of their action. Such an approach has proved to be successful in clarifying the formation of the spectral line component of the noise attributed to solar active regions.

We have applied our model to ground based velocity measurements, comparing our results with the data obtained by the IRIS network, and we plan to extend the simulation for calibrating the data coming from the GOLF experiment, whose level of background noise is expected to be one order of magnitude lower than it is on ground based measurements.

Preliminary results of our simulation have been presented by Marmolino et al. (1995, hereafter Paper I). In this paper we complete the analysis started in Paper I discussing in details the dependence of the simulation results upon a number of model parameters. Specifically, in Sect. 2 we recall the methods and describe the data which our simulation is based on; in Sect. 3 we review briefly on the calibration methods necessary to get velocities out of the observed photometric ratios; in Sect. 4 we show and discuss the results, and in Sect. 5 we summarize our main conclusions.

2. Methods

Our approach was originally motivated by the aim to simulate the possible detection of g - modes by a Na I resonance spectrometer, like the one proposed for the GOLF experiment on board of SOHO, or those in use by the IRIS network. Therefore, we planned to follow this scheme:

- develop wave models for gravity modes in the solar atmosphere expanding the work of Marmolino et al. (1991, 1993) with the inclusion of a temperature stratified atmosphere with spherical symmetry;
- add the wave model to a standard reference atmosphere of the Quiet Sun to produce a grid of perturbed

solar models, which account for the effective conditions meet by radiation during a wave period;
- calculate the synthetic profiles of the Na I D lines over the grid, and integrate them over the disk to produce the flux profile F_λ;
- finally determine the photometric ratio r measured by a resonance spectrometer, i.e.

$$r = \frac{F_\mathrm{b} - F_\mathrm{r}}{F_\mathrm{b} + F_\mathrm{r}} \quad (1)$$

where F_b and F_r represent the flux in blue and red working points of the spectrometer, respectively.

The interaction with the GOLF community has stimulated us to afford first of all the problem of solar noise, and, for this work, we have modified the scheme outlined above in the first two items that became

- determine the spatial distribution of active regions over the solar disk for a period lasting more rotation periods;
- produce a grid of active regions models which account for the effective conditions meet by radiation in the different solar magnetic structures.

We assume that active regions consist of two components, a warmer structure or plage and a cooler structure or spot. Let us discuss how the daily distribution of spots and plages over the solar disk has been determined.

2.1. Active region data

For the period from June 10, 1990 to November 29, 1991, the daily distribution of spots and plages over the disk has been determined from the Ca II K line full disk archive of the Big Bear Solar Observatory.

For example, in Fig. 1, we show the K line image of the Sun for February 1, 1991 from BBSO, and the distribution we have inferred for plages and spots, after removing the center-to-limb variations. To get the active region areas, we used as contrast thresholds an upper bound of 0.8 for spots, and a lower bound of 1.3 for plages. However, because the fraction of solar disk covered by plages depends strongly on the latter threshold, in Sect. 4 we report also on results obtained with a plage lower bound of 1.15.

Note that eventually we used only the images from August 1 to November 29, 1991 for comparison with IRIS, because in this period the IRIS offset velocities have the minimum scatter, and also the BBSO archive has a gap from August to December 1990 as a result of the well-known earthquake.

2.2. Atmospheric models and sodium line formation

As model atmosphere for the quiet Sun we have selected model C of Fontenla et al. (1993). The spot model was the version of the Maltby et al. (1986) umbral model modified by Severino et al. (1994). Finally, the plage model is one of the active region models developed by Andretta & Giampapa (1995). Following the approach of Cram & Mullan (1979), these models have been built by shifting inward the temperature structure, by a fixed amount $\Delta \log m$, where m is the mass column density (in g cm^{-2}) of the quiet atmosphere. In particular we used the model corresponding to $\Delta \log m = 0.7$ (hereafter called PLAGE07). Moreover, we shifted inward of the same amount also the microturbulence structure. As shown by Severino et al. (1993), we selected this particular plage model, because, in this way, it is possible to reproduce the "antiplage" behaviour observed in the sodium D_1 line at about 100 mÅ from the line center, (Ulrich et al. 1993). Otherwise, when the sodium line is computed with the Fontenla et al. model atmosphere for plage, the plage appears bright at the working points of a sodium cell (e.g. Fig. 3 of Paper I). However we remark that the agreement we got between computed and observed plage contrasts is qualitative, and in Sect. 4 we will allow for a number of different contrasts (see Figs. 6 and 7).

Finally, we used the version 2.0 of the code MULTI of Mats Carlsson (1986) for the NLTE sodium line synthesis; more details on this are given in Sect. 2 of Paper I.

2.3. Flux determination

Since the velocity measures refer to low degree modes, we have to integrate the emergent intensity over the entire disk to find the flux in the sodium line, accounting for the three-component time dependent distribution of the intensity over the disk. We performed the flux integration analytically, which allowed us to have more insight into results. However, we checked that for a number of different distributions of spots over the disk the analytical method produces velocity fluctuations which agree within 5% with the results of the direct numerical integration.

The analytical formulation of the irradiance variations produced by active regions was extensively developed in Sect. 3 of Paper I. The final result of that section was that, with the assumptions that the disk is covered by a discrete distribution of active regions with a contrast depending only upon the heliocentric angle, and that the emergent intensity can be adequately represented by the linear terms in the solar rotational velocity, we can write the emergent flux at wavelength λ as

$$F(\lambda) = F^\mathrm{q}(\lambda + \delta\lambda_0) + \delta F_0(\lambda + \delta\lambda_0) + \delta F_\mathrm{r}(\lambda + \delta\lambda_0) \quad (2)$$

where $F^\mathrm{q}(\lambda+\delta\lambda_0)$ is the flux emergent from the quiet disk, broadened by solar rotation and shifted by $\delta\lambda_0$ because of the relative velocity V_0, which includes the Sun-Earth relative motions and the gravitational redshift; the other two terms represent the modulations due to the active regions, with $\delta F_0(\lambda + \delta\lambda_0)$ independent of the solar rotation, and $\delta F_\mathrm{r}(\lambda + \delta\lambda_0)$ at the first order in the rotation velocity. Both these terms can be expressed by summations over

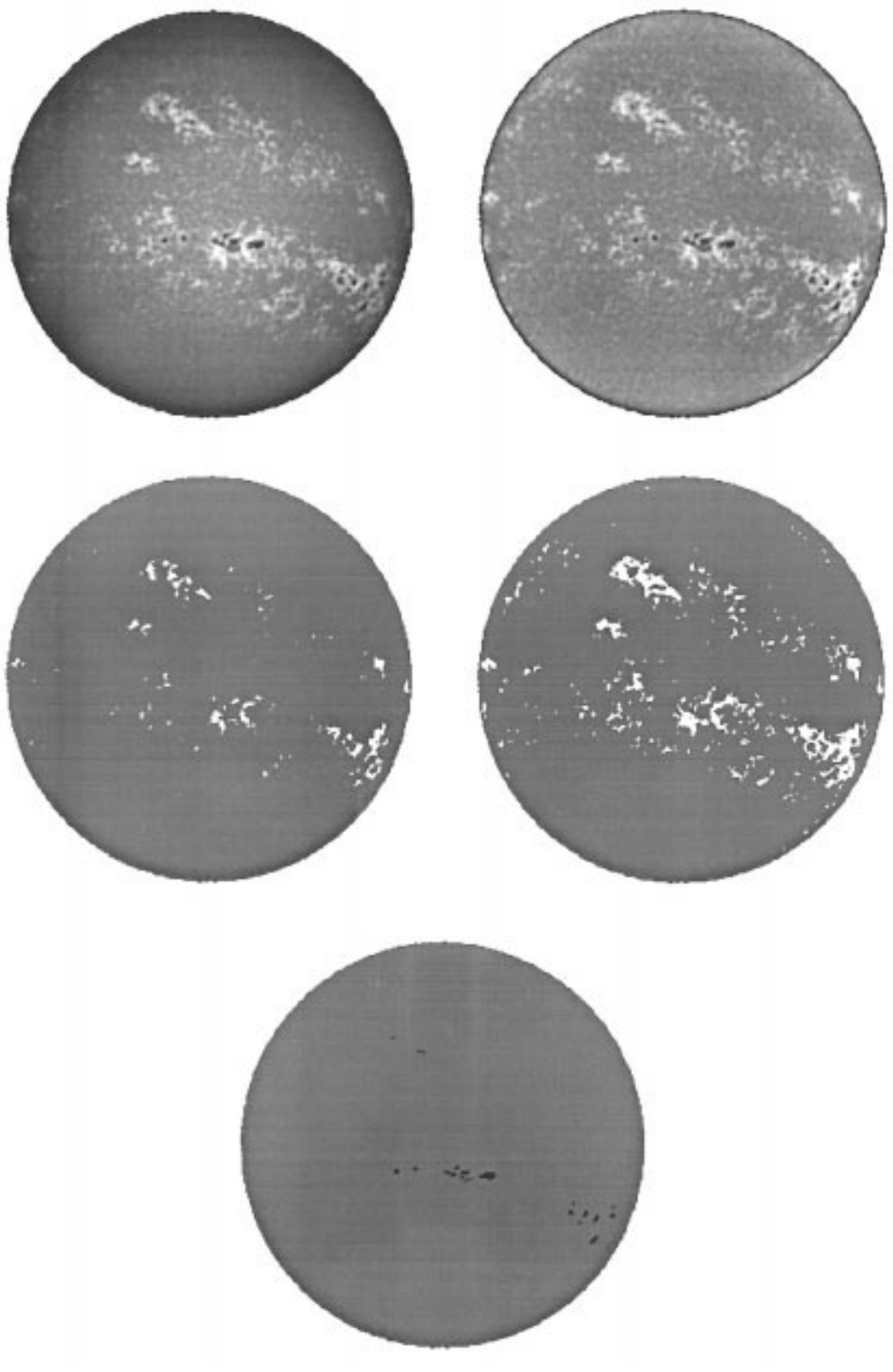

Fig. 1. Distribution of active regions over the solar disk on February 1, 1991. From left to right, and top to bottom: CaII K line image from the Big Bear Solar Observatory; the same image with the center-to-limb variations removed; inferred plage distributions obtained with a lower bound for the plage contrast of 1.30 and 1.15 respectively; inferred spot distribution used for the simulation. The total projected area covered by spots is 0.27 percent of disk, and that covered by plages is 1.5% and 5.7% respectively

the active regions effectively present on the disk as (see also Livingston et al. 1991)

$$\delta F_0 = 2\pi \sum_i A_i \mu_i I^{\rm q}(\lambda + \delta\lambda_0, \mu_i) \left[C_i(\lambda + \delta\lambda_0, \mu_i) - 1\right] \quad (3)$$

$$\delta F_{\rm r} = \frac{\lambda_0}{c} 2\pi \sum_i A_i V_{\rm r}(\mu_i, \phi_i) \mu_i \quad (4)$$

$$\frac{\rm d}{{\rm d}\lambda} \left\{ I^{\rm q}(\lambda + \delta\lambda_0, \mu_i) \left[C_i(\lambda + \delta\lambda_0, \mu_i) - 1\right] \right\}$$

where A_i is the area (in units of solar hemisphere), $I^{\rm q}$ is the emergent intensity of the quiet Sun, C_i denotes the contrast of the $i^{\rm th}$ active region located at distance $\sqrt{1-\mu_i^2}$ from the disk center and with azimuth ϕ_i, and $V_{\rm r}(\mu_i, \phi_i)$ is the line-of-sight component of the rotational velocity.

Once the active region distribution is known from the K line daily images, and the relative velocity is determined according to the ephemerides, we can compute the fluxes in the blue and red flanks of the sodium D_1 line from Eqs. (2), (3) and (4), and then we can determine the photometric ratio r according to Eq. (1).

3. Calibration in velocity

The passage from the photometric ratio r to a velocity is not trivial, but requires a calibration procedure which has been argument of many papers reporting oscillation measures from resonant spectrometers (see e.g. van der Raay et al. 1985; Pallé et al. 1993).

3.1. Standard procedure

The calibration is based on a best fitting procedure of the relation $r = f(V)$, where V represents a total line of sight velocity. The difficulties arise since the velocity V is partly unknown and partly spurious. In effect, according to Pallé et al. (1993), we can write

$$V = V_{\rm osc} + V_{\rm off} + V_0$$

where $V_{\rm osc}$ is the unknown solar oscillation velocity, $V_{\rm off}$ is an unknown solar offset, and V_0 is the known part of V. $V_{\rm off}$ includes the integrated signal produced by the active region as well as by the solar velocity fields at different scales. Pallé et al. claim that $V_{\rm off}$ is roughly constant during a 12-hour observation ($\Delta V_{\rm off} \leq 2$ m s^{-1}) while it changes by as much as 20 m s^{-1} in 7 days. In the case of ground-based measurements, V_0 is

$$V_0 = V_{\rm spin} + V_{\rm orbit} + V_{\rm atm} + V_{\rm gra}$$

where the first two terms are due to Earth-Sun relative motion, $V_{\rm atm}$ is the signal produced by the Earth atmosphere differential extinction, and $V_{\rm gra}$ is the gravitational redshift in velocity unit (639 m s^{-1}). In the case of the GOLF measurements, V_0 is

$$V_0 = V_{\rm orbit} + V_{\rm halo} + V_{\rm gra}$$

where $V_{\rm halo}$ is the component relative to the satellite halo orbit around the Lagrangian point L_1, and $V_{\rm orbit}$ is the same as for ground-based observation with the approximation that the Lagrangian point is placed at the Earth position. In both cases, V_0 can be calculated with great accuracy.

The calibration procedure developed by Pallé et al. (1993) for the IRIS data consists of two steps: i) first a table $r_{\rm m}$ vs. V_0 was built, where $r_{\rm m}$ is the mean of r over 1 m s^{-1} bins of V_0, in which the variations of $V_{\rm osc}$ and $V_{\rm off}$ are minimized, and an average calibration function $f(V) = r_{\rm m}$ was determined by fitting the function $f(V) = \frac{A_{\rm m}V + B_{\rm m}}{1+\alpha V^2+\beta V^4}$ to the table $r_{\rm m}$ vs. V_0; ii) the α and β coefficients derived in the previous step are used to calculate the linearized ratio $r' = r(1 + \alpha V^2 + \beta V^4)$; and then the fit of r' vs. $V_{\rm spin}$ to the straight line $AV + B$ for each observing day provides the daily varying sensitivity A and offset B.

3.2. Crossed method

Boumier et al. (1994) discussed a method of analyzing data in the case of a resonant spectrometer sampling the sodium line profiles at 4 points, 2 in the red wing and 2 in the blue wing. A 4-point spectrometer is realized by modulating the instrumental magnetic field B by a small amount δB around its working value (Isaak & Jones 1988). In this case, it is possible to define the two crossed ratios $0^+ = \frac{F_{\rm b+} - F_{\rm r-}}{F_{\rm b+} + F_{\rm r-}}$, and $0^- = \frac{F_{\rm b-} - F_{\rm r+}}{F_{\rm b-} + F_{\rm r+}}$, with the opposite signs denoting the two magnetic configurations $B + \delta B$ and $B - \delta B$. The calibration, $C_{\bar r} = V(\bar r)/\bar r$, is defined in terms of the average ratio $\bar r = (r(B^+) + r(B^-))/2$, and is obtained from $C_{\bar r} = \frac{\delta V_B}{\bar r} \frac{0^+ + \beta 0^-}{0^+ - \beta 0^-}$, where δV_B is the velocity displacement corresponding to the magnetic modulation, and $\beta = \frac{0^+}{0^-} \frac{V(0^-)}{V(0^+)}$. Rigorously, the coefficient β depends on the observed velocity itself, and then has to be estimated to carry on the procedure. To follow the time evolution of $C_{\bar r}$, Boumier et al. fit the calibration factor with a 9th order polynomial on their one day dataset.

Looking at the expression of $C_{\bar r}$, we note that its main time dependence comes from the inverse dependence on $\bar r$, because it is $\frac{0^+ + \beta 0^-}{0^+ - \beta 0^-} = \frac{1 + \beta 0^-/0^+}{1 - \beta 0^-/0^+}$, and $\beta \frac{0^-}{0^+} = \frac{V(\bar r) - \delta V_B}{V(\bar r) + \delta V_B}$ (see Boumier et al. 1994, their Eq. (8)). In fact, in our simulation of the IRIS offset velocities we have experimented the crossed method, following the whole time evolution of $C_{\bar r}$ from August 1 to November 29, 1991, and we got the result that the active region signal was essentially canceled by this calibration. Therefore, in our opinion, one should apply to the crossed method the caution that the higher the order of the polynomial representing the calibration factor, the more precise the observed velocity fit, but also

the higher the filtering probability of possible signals, as, on the other hand, Boumier et al., in the same paper, have stated for the polynomial method and the 2-point measure.

Eventually, we have selected for our simulation a calibration method, which is based on the Pallé et al. calibration procedure with one main difference: on one hand, we have at disposal only one ratio per day, because there is one solar image in the CaII K line per day, and, on the other hand, we have the possibility to build the ratio r_q corresponding to the Sun *without* active regions; therefore, we fit directly the calibration function $f(V) = \frac{\bar{A}V+\bar{B}}{1+\alpha V^2+\beta V^4}$ to the table r_q vs. V_0.

In conclusion, we emphasize that it is important to understand and model the different causes of solar noise in order to remove them directly without the risks inherent in methods based essentially on data smoothing. In other words, the best approach to calibration is to reduce as much as possible the unknown part of the velocities used for calibration.

4. Results

4.1. The ar-rv effect

In Fig. 2, we plot the results of our simulation of the offset velocities measured by IRIS, for the period from August 1 to November 29, 1991. In this case, we got a constant calibration factor with a value of $A^{-1} = 3673.3$ m s^{-1}.

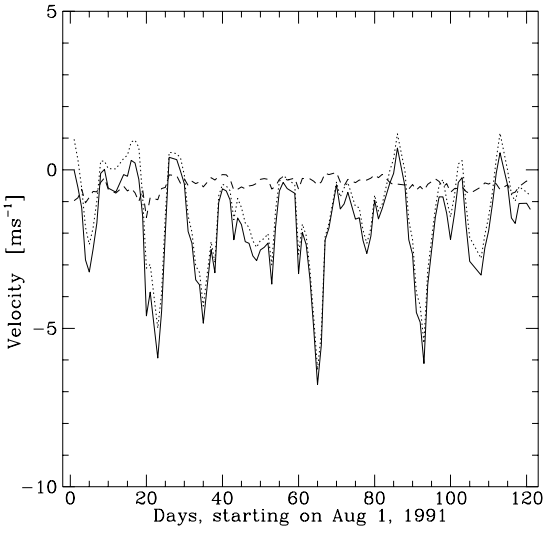

Fig. 2. Simulated velocity vs. time for the period from August 1 to November 29, 1991, and for the IRIS measurement. Solid line is the signal produced by the active regions; dotted line is the signal obtained with zero relative velocity, i.e. by fixing the passbands of the cell at ±95 mÅ during the full period, and dashed line represents the difference between these two signals

In our model, the magnetic darkening velocity are modulated not only by the solar rotation rate, but also by the Sun-instrument relative velocity, because the latter controls the effective position of the cell working points. In fact, there is a contribution to the computed velocity produced by the combined presence of both the active regions and a non-zero relative velocity, with the active regions changing the shape of the sodium line and the relative velocity making the instrumental response to this change different on the red and blue flanks of the line. This velocity, which is independent of the solar rotational velocity, and whose amplitude is of the order of one m s^{-1}, was called in Paper I the *active region-relative velocity effect* (hereafter, ar − rv effect).

Because the relative velocity (Earth rotation plus gravitational redshift) varied between a maximum of 437 m s^{-1} (on August 1) and a minimum of 140 m s^{-1} (on October 5), during the observing period the center of the red (blue) cell passband moved within the range from +98 to +108 (−108 to −98) mÅ (in separation from the D_1 line center).

In Fig. 2, we plot also the signal simulated with zero relative velocity, that was computed by fixing the working points of the cell at ±95 mÅ during the full period, and the difference between the signals simulated *with* and *without* relative velocity. This difference can be produced by the ar − rv effect, and by any E − W asymmetry of the active region distribution. Because the Sun was very active at that time, we would expect a shorter time scale for the asymmetry effect than for the ar − rv effect. In fact, the general trend of the difference is of the order of 1 m s^{-1}, negative and slightly decreasing in time towards October; both the sign and the trend are consistent with the ar − rv effect (see Paper I), since the relative velocity is positive during the period under examination, and has its minimum in October; moreover it can be shown that it is essentially connected with plages, which have larger areas and a larger ar − rv effect than spots. As a result, the signal simulated in the presence of a non-zero relative velocity is generally negative (the mean is −1.5 m s^{-1}), and velocity deeps are generally sharper than peaks.

4.2. Plage/spot contributions

Figure 3 shows the separate contribution of plages and spots to the total velocity signal produced by active regions in our simulation. Generally, the two trends are similar, i.e. they show most of the same peaks and dips at the same days; this is a consequence of both the location of the plages, which occur around the spots, and of the *antiplage* character of the plage contrast in the Na I D_1 line flanks. As already stated in Paper I, it appears that plages give the dominant contribution; the rms contribution of spots to total velocity fluctuations is not negligible. It is not easy to understand why this result holds, because also with the approximation that only the term δF_r is affecting the ratio r, there are the mixed influences of the active region

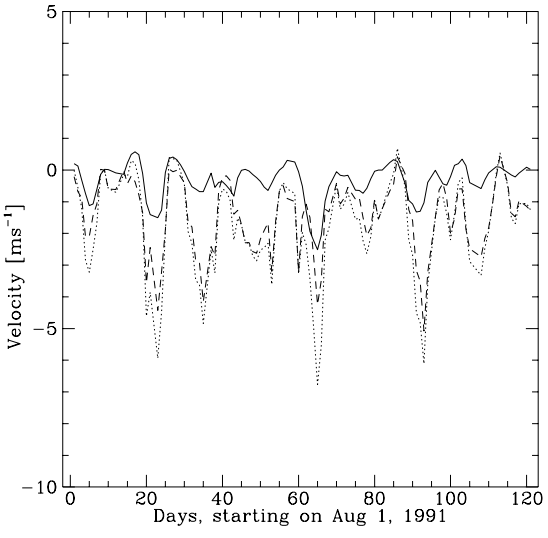

Fig. 3. Simulated velocity vs. time for the period from August 1 to November 29, 1991, and for the IRIS measurement. Dotted line is the signal produced by the active regions; while solid and dashed lines are the contributions of plages and spots to the total velocity, respectively

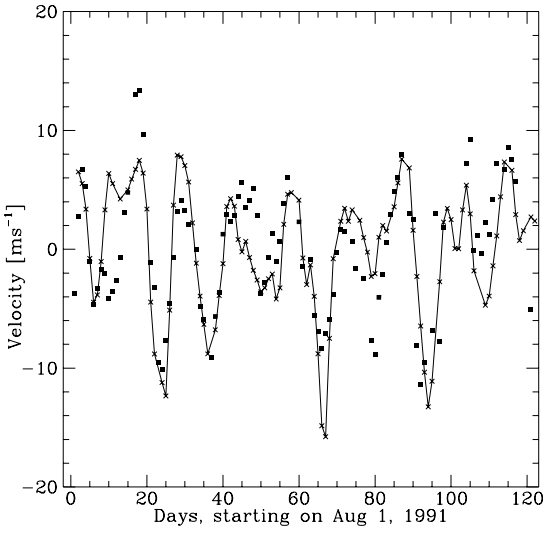

Fig. 4. Velocity fluctuation vs. time for the period from August 1 to November 29, 1991: solid line is the signal produced by our simulation, multiplied times the factor 3.6, and the full squares represent the IRIS offset velocities

areas and contrasts with their dependences on wavelength (see Eq. 4). Obviously, the plage contribution to the total simulated signal is even more enhanced when the intensity threshold used to determine the plage areas is lowered.

4.3. Comparison with IRIS

In Fig. 4, we compare our simulation with the IRIS data. Our calculation has been detrended for the ar − rv effect, which, at least partly, calibration may have already canceled in the observed data. They have also been scaled with the ratio of the observed to calculated rms velocity amplitude, $\frac{<v_{\rm obs}>_{\rm rms}}{<v_{\rm cal}>_{\rm rms}} = 3.6$, which is analogous to the saturation factor used by Ulrich et al. (1993). A value of the saturation factor larger than unity is partly explained by the high value of the IRIS calibration, about 8000 m s^{-1}, with respect to ours, 3673 m s^{-1}. The calibration of the IRIS instrument at Tenerife in 1991 was high because of both instrumental unresonant diffused light and imperfect performance of the circular analysers.

Moreover, since the IRIS velocities are daily means (and we assume noon as the mean observation time), while BBSO images have exposure times of few seconds (usually obtained between 3 and 6 pm), we applied a two point smoothing to our simulation.

We measure the goodness of the fit by two quantities, the correlation coefficient $t_{\rm corr}$ between computed and observed velocities, and the residual relative amplitude $A_{\rm rr} = \frac{<v_{\rm cal}-v_{\rm obs}>_{\rm rms}}{<v_{\rm obs}>_{\rm rms}}$, which is equal to the square root of the variance ratio used by Ulrich et al. (see their Fig. 13); we shifted in time the computed velocities by a quantity $t_{\rm scale}$ in order to maximize $t_{\rm corr}$ and minimize $A_{\rm rr}$, however we found that it is easier to increase the correlation than to reduce the residual relative amplitude. The comparison reported in Fig. 4 has $t_{\rm corr} = 0.71$ and $A_{\rm rr} = 0.78$; all observed peaks and dips are present also in the simulation, and during specific periods (e.g. from September 1 to 30), the fit is strikingly good. On this base we consider the agreement between our simulation and the IRIS data as rather good; however if we subtract our calculations from the data, the residual fluctuation is about 4 m s^{-1}, i.e. twice the mean error we may ascribe to the data as inferred from a comparison between the velocities obtained at Kumbel and Tenerife during the same period (see Fig. 8 of Pallé et al. 1993). Therefore, not differently from Ulrich et al., we conclude that our ability to simulate the IRIS offset velocities is not yet enough, and the use of the present approach as a standard correction procedure to remove the active regions noise deserves a refinement of the simulation as well as more than one observing dataset to compare with.

Possible changes in the parameters of our simulation to reduce the discrepancies with the IRIS data are described in the following chapter; while a critical discussion of the ingredients of our model and of the possible future improvements is given in Sect. 5.

4.4. Sensitivity to different parameters

The parameters upon which our simulation depends can be inferred from the inspection of Eqs. (1)-(4): the intensity thresholds used for the analysis of the K line images determine the areas of spots and plages, as described in

Sect. 3. The contrast of the active regions is obviously relevant, and, finally, there is the effect of the relative velocity V_0, entering through the ar − rv effect.

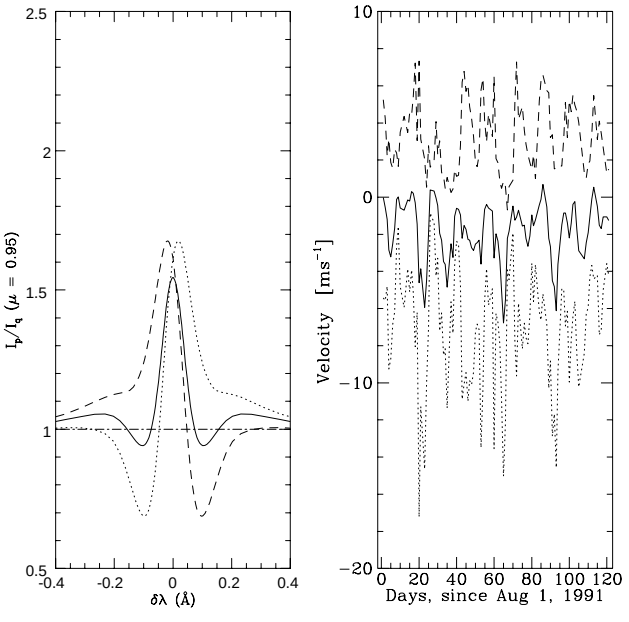

Fig. 5. Sensitivity of the simulation to changes in V_0. Solid line is the signal produced by our simulation, while dotted and dashed lines correspond to a change of -400 m s^{-1} and $+400$ m s^{-1}, respectively

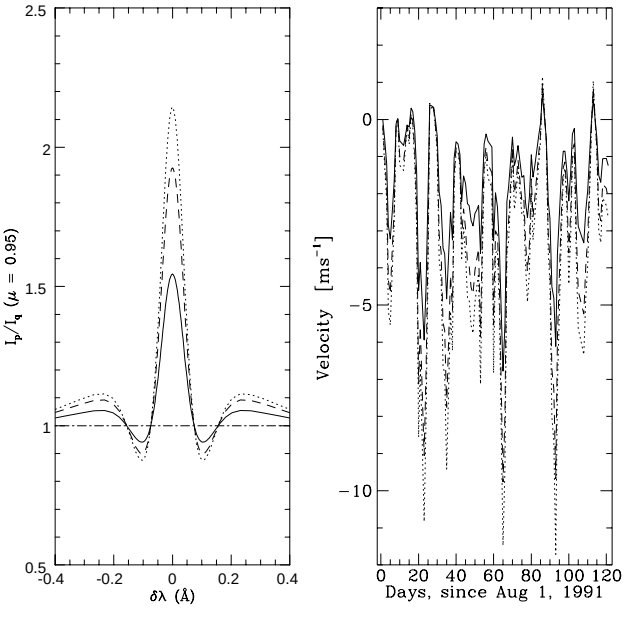

Fig. 6. Sensitivity of the simulation to changes in the strength of the plage contrast. Each velocity curve in the right panel corresponds to the contrast plotted with the same linetype in the left panel

We ran a simulation with a lower bound for the plage contrast (15% instead of 30%); this more than doubles the area covered by plages. The general trend of the simulated signal, as shown in Fig. 4, is present also in this case, with the a reduction from 3.6 to 1.2 of the saturation factor, needed to match the observed amplitudes.

Figure 5 shows the sensitivity of the simulation to changes in V_0. The general trend of the simulated signal is not changed by a constant variation of the relative velocity of ± 400 m s^{-1}. However, it has to be noted that we assumed that each IRIS datum refers to noon, and then we neglected the contribution of the line-of-sight component of the Earth spin in the relative velocity, i.e. $V_{\rm spin} = 0$. Because the tables of the IRIS observing times were not at our disposal, we cannot rule out that the average of $V_{\rm spin}$ during some observing days may be not zero; therefore. our incomplete knowledge of V_0 is a possible source of errors in the simulation, which might change sharply from one day to the next.

In Fig. 6, we show the sensitivity of the simulation to a variation in strength of the plage contrast. An inspection of Fig. 1 in Ulrich et al. (1993) indicates that our synthetic plage contrast is smaller than the observed one by a factor up to 1.7 at the cell working points. An underestimate of the plage contrast and areas partly explains the value of 3.6 of our saturation factor. We ran a number of simulations with increasing plage contrasts; the results show again that peaks and dips of the simulated signal are emphasized with respect to the result with standard contrast, but their locations and shapes are substantially unmodified.

The same conclusion does not apply when we make the plage contrast asymmetric by shifting the plage relative to quiet Sun line profile, as it is illustrated in Fig. 7. In fact, in the simulations considered so far, we did not include the contribution of intrinsic velocities of the active regions; while there are both observations and theoretical reasons supporting the existence of motions in active regions, and, hence, of Doppler shifts in particular between the plage and the quiet Sun profiles. Moreover, convection produces line shifts, which may be different in the quiet and active areas of the Sun; e.g. in the case of Na I D_1 and at the working points of the IRIS, the absolute line shift should be of about 50 m s^{-1} (1 mÅ), at the quiet solar disk center (Boumier 1991).

The two cases reported in the figure, which correspond to a ± 20 mÅ shift between the plage relative to quiet Sun line profile, are somewhat extreme (in fact, a 20 mÅ shift in a circularly polarized component of the Na I D_1 line may be produced by a downdraft of 1 km s^{-1}); however, also by running simulations with half this value for the plage line shift, it is apparent that the inclusion of intrinsic

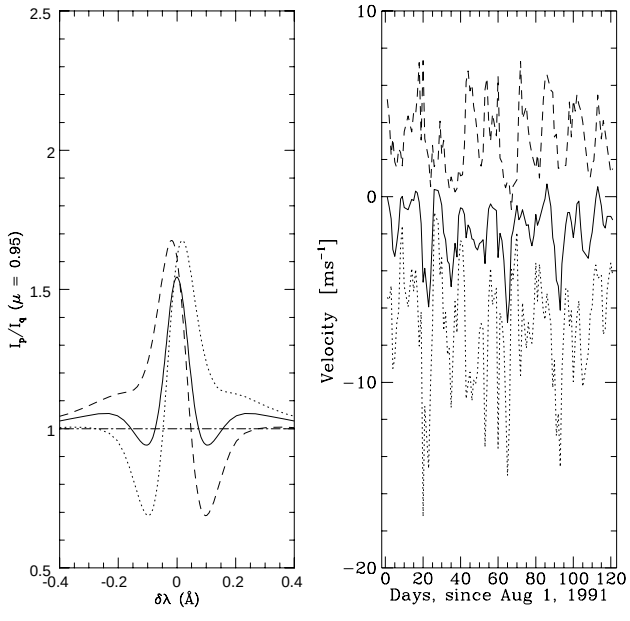

Fig. 7. Sensitivity of the simulation to shifts of the plage relative to quiet Sun line profile. Each velocity curve in the right panel corresponds to the contrast plotted with the same linetype in the left panel

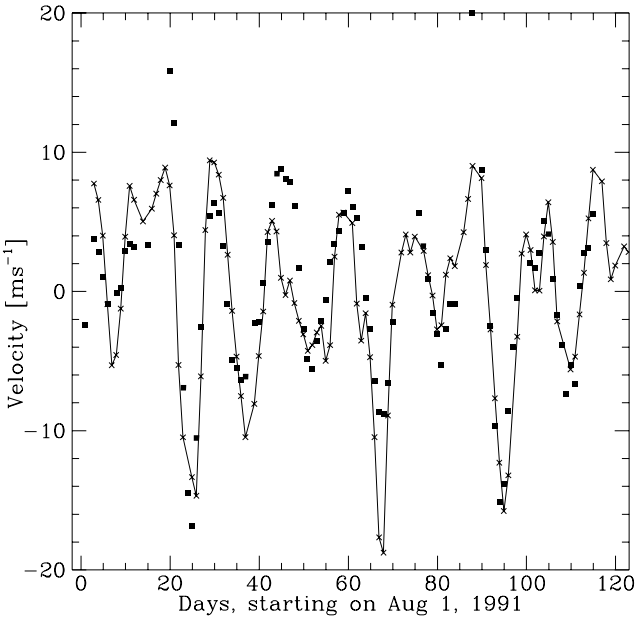

Fig. 8. Velocity fluctuation vs. time for the period from August 1 to November 29, 1991. Solid line is the signal produced by our simulation, multiplied times the factor 4.3, and the full squares represent the results of the simulation from Ulrich et al. (1993)

line shifts can change strongly not only the amplitude of the simulated signal but also the shapes of peaks and dips, and then may be an important source of uncertainty for the simulation.

4.5. Comparison with another simulation

We compare our simulation with the one of Ulrich et al. (1993) in Fig. 8. The Ulrich et al. simulation is based on the distribution of the longitudinal magnetic field as obtained from the daily Mount Wilson magnetograms, and on an empirical correlation between the value of this magnetic field and the darkening in the flanks of the Na I D_1 line. The quantitative comparison of the two simulations give a correlation of 0.79 and a residual relative amplitude of 0.72. Both these values are slightly better than those obtained by comparing our simulation with the IRIS data (0.71 and 0.78 respectively), however this does not seem to have a particular meaning. The major difference between the two simulations is in the fact that Ulrich et al. defined the active regions in terms of the longitudinal magnetic field, whilst we do that according to the intensity in the Ca II K line core. In fact, one would expect that the plage brightening does not strictly "remake" the magnetic field distribution; also, the longitudinal field may become a poor description of the active regions close to limb. On the other hand, Ulrich et al. allow for a continuous range of values of the magnetic darkening, whilst we consider only a two component (spot-plage) distribution. In spite of these differences, both simulations have essentially the same ability in reducing the observed offset velocity fluctuations, since from Fig. 13 of Ulrich et al. we infer a best residual variance close to 0.6, and then a residual relative amplitude of 0.77, which is very close to ours.

5. Conclusions

We presented a simulation of the spurious velocities that active regions can produce in the measurement of the global Sun velocity with a resonance scattering spectrometer. The simulation is based on the spot and plage areas inferred from the BBSO CaII K line filtergrams, and on the sodium line profiles computed numerically in active regions model atmospheres.

In the simulation, plages play the major role in determining the spurious velocities. The relative velocity affects the spurious velocities at 1 m s^{-1} level through the ar − rv effect. The simulation allows to test calibration procedures and to study the effect of different parameters on the spurious velocities. However, its ability to fit the offset velocities observed by the IRIS project, even if rather good, is not yet enough, and the use of the present approach as a standard correction procedure to remove the active regions noise deserves a refinement of the simulation as well as more than one observing dataset to compare with. The simulated velocities show a general agreement with the

observations, but cannot reproduce with the same precision different observation days: the error is random.

We think that the simulation could be improved notably by using a more detailed representation of the plage contrast, to take into account that there is a distribution of plages on the disk with different contrasts or, also, there are large plages with a contrast spatially variable.

Furthermore, it will be useful to include in the model convective effects associated with plage areas, that can alter the plage contrast by shifting the plage profile with respect to the quiet Sun. A confirm might be considered the fact that the mean of all the simulation we ran with different parameters (V_0 variations, smoothing time, cell passbands, plage contrast and shift) give the best correlation (0.76) and the best residual relative amplitude (0.68, i.e. variance 0.46).

In perspective, the methods presented in this paper will be used for an improved simulation based on the Doppler and Magnetic images collected by a MOF which is in course of implementation at the Osservatorio Astronomico di Capodimonte, in collaboration with A. Cacciani e P.F. Moretti (Dip. Fisica, Univ. La Sapienza, Roma).

Acknowledgements. It is a pleasure to thank Eric Fossat and Roger Ulrich who made available to us their data. Also, we thank Thomas Straus for reading the manuscript, the anonymous referee, and Jean Maurice Robillot, as second referee, for their helpful comments. This work was partially supported by the Italian Space Agency (ASI).

References

Andersen B.N., Leifsen T., Toutain T., 1994, Solar Phys. 152, 247
Andersen B.N., Maltby P., 1983, Nat 302, 808
Andretta V., Giampapa M.S., 1995, ApJ 331, 211
Beck J.G., Ulrich R.K., Hill F., 1995, in GONG'94: Helio- and Asteroseismology from Earth and Space, Ulrich R.K., Rhodes E.J Jr. & Däppen W. (eds.). ASP Conf. Ser. 76, 296
Boumier P., 1991, PhD Thesis, Université de Paris VII
Boumier P., van der Raay H.B., Roca Cortés T., 1994, A&AS 107, 177
Carlsson M., 1986, A Computer Program for Solving Multi-Level Non-LTE Radiative Transfer Problems in Moving or Static Atmospheres, Report No. 33, Uppsala Astronomical Observatory
Claverie A., Isaak G.R., McLeod C.P., et al., 1982, Nat 299, 704
Cram L.E., Mullan D.J., 1979, ApJ 234, 579
Dicke R.H., 1983, Nat 303, 292
Durrant C.J., Schröter E.H., 1983, Nat 301, 589
Edmunds M.G., Gough D.O., 1983, Nat 302, 810
Elsworth Y., Howe R., Isaak G., et al., 1993, in GONG 1992: Seismic Investigation of the Sun and Stars, Brown R.M. (ed.). ASP Conf. Ser. 42, 107
Fontenla J.M., Avrett E.H., Loeser R., 1993, ApJ 406, 319
Fossat E., 1991, Solar Phys. 133, 1
Gabriel A., et al., 1995, Solar Phys. 162, 61
Harvey J.W., 1985, in Future Missions in Solar, Heliospheric and Space Plasma Physics, Rolfe E.J. & Battrick B. (eds.). ESA SP-235, p. 199
Harvey J.W., Duvall Jr. T.L., Jefferies S.M., Pomerantz M.A., 1993, in GONG 1992: Seismic Investigation of the Sun and Stars, Brown T.M. (ed.). ASP Conf. Ser. 42, 111
Harvey J.W., 1995, in Fourth Soho Workshop Helioseismology, Hoeksema T.J., Domingo V., Fleck & Battrick B. (eds.). ESA SP-376 1, 9
Herrero A., Jimenez R., Roca Cortés T., 1984, Mem. S. A. It. 55, 331
Isaak G.R., van der Raay H.B., Pallé P.L., Roca Cortés T., 1984, Mem. S. A. It. 55, 339
Isaak G.R., Jones A.R., 1988, in Advances in Helio- and Asteroseismology, Christensen-Dalsgaard J. & Frandsen S. (eds.) p. 211
Jiménez A., Pallé P.L., Pére Hernández F., Régulo C., Roca Cortés T., 1988, A&A 192, L7
Jiménez A., Pallé P.L., Régulo C., et al., 1988, in Advances in Helio- and Asteroseismology, Christensen-Dalsgaard J. & Frandsen S. (eds.) p. 211
Livingston W.C., Donnelly R.F., Grigoryev V., et al., 1991, in The Solar Interior & Atmosphere, Cox A.N., Livingston W.C. & Matthews M.S. (eds.). The University of Arizona Press, Tucson, p. 1109
Maltby P., Avrett E.H., Carlsson M., Kjeldseth-Moe O., Kurucz R.L., Loeser R., 1986, ApJ 306, 284
Marmolino C., Oliviero M., Severino G., Smaldone L.A., 1995, in Fourt Soho Workshop Helioseismology, Hoeksema T.J., Domingo V., Fleck B. & Battrick B. (eds.), ESA SP-376 2, 407 (Paper I)
Marmolino C., Severino G., 1991, A&A 242, 271
Marmolino C., Severino G., Deubner F.-L., Fleck B., 1993, A&A 278, 617
Pallé P.L., Fossat E., Régulo C., et al., 1993, A&A 280, 324
Régulo C., Pallé P.L., Roca Cortés T., 1993, in Vth IRIS workshop & GOLF'93 annual meeting, Roca Cortés T. (ed.). IAC Tenerife Spain, p. 69
Severino G., Andretta V., Gomez M.T., Marmolino C., 1993, in Vth IRIS workshop & GOLF'93 annual meeting, Roca Cortés T. (ed.). IAC Tacoronte, Tenerife, p. 63
Severino G., Gomez M.T., Caccin B., 1994, in Solar Surface Magnetism, Rutten R.J. and Schrijver C.J. (eds.). NATO ASI Ser. C 433, p. 169
Thomson D.J., Maclennan C.J., Lanzerotti L.J., 1995, Nat 375, 13 July 1995
Ulrich R.K., Henney C.J., Schimpf S., et al., 1993, A&A 280, 268
van der Raay H.B., Pallé P.L. Roca Cortés T., 1985, in Seismology of the Sun & the Distant Stars, Gough D.O. (ed.). Reidel, Dordrecht, p. 333